

Accepted Manuscript

Verapamil and riluzole cocktail liposomes overcome pharmacoresistance by inhibiting P-glycoprotein in brain endothelial and astrocyte cells: A potent approach to treat amyotrophic lateral sclerosis

Tianzhi Yang, Laine Ferrill, Leanne Gallant, Sarah McGillicuddy, Tatiana Fernandes, Nicole Schields, Shuhua Bai



PII: S0928-0987(18)30191-X

DOI: doi:[10.1016/j.ejps.2018.04.026](https://doi.org/10.1016/j.ejps.2018.04.026)

Reference: PHASCI 4489

To appear in: *European Journal of Pharmaceutical Sciences*

Received date: 30 December 2017

Revised date: 3 April 2018

Accepted date: 18 April 2018

Please cite this article as: Tianzhi Yang, Laine Ferrill, Leanne Gallant, Sarah McGillicuddy, Tatiana Fernandes, Nicole Schields, Shuhua Bai , Verapamil and riluzole cocktail liposomes overcome pharmacoresistance by inhibiting P-glycoprotein in brain endothelial and astrocyte cells: A potent approach to treat amyotrophic lateral sclerosis. The address for the corresponding author was captured as affiliation for all authors. Please check if appropriate. Phasci(2017), doi:[10.1016/j.ejps.2018.04.026](https://doi.org/10.1016/j.ejps.2018.04.026)

This is a PDF file of an unedited manuscript that has been accepted for publication. As a service to our customers we are providing this early version of the manuscript. The manuscript will undergo copyediting, typesetting, and review of the resulting proof before it is published in its final form. Please note that during the production process errors may be discovered which could affect the content, and all legal disclaimers that apply to the journal pertain.

Verapamil and riluzole cocktail liposomes overcome pharmacoresistance by inhibiting P-glycoprotein in brain endothelial and astrocyte cells: a potent approach to treat amyotrophic lateral sclerosis

Tianzhi Yang, Laine Ferrill, Leanne Gallant, Sarah McGillicuddy, Tatiana Fernandes, Nicole Schields, and Shuhua Bai*

Department of Basic Pharmaceutical Sciences, School of Pharmacy, Husson University,
1 College Circle, Bangor, ME 04401

* To whom all correspondence should be addressed:

Phone: 001-207-992-1949, Fax: 001-207-992-1954

E-mail: BaiS@husson.edu

Running title: P-gp inhibition by verapamil and riluzole cocktail liposomes

Abstract

Riluzole is currently one of two approved medications for the treatment of amyotrophic lateral sclerosis (ALS). However, brain disposition of riluzole, as a substrate of P-glycoprotein (P-gp), is limited by the efflux transporters at the blood-brain barrier (BBB). We propose to develop a liposomal co-delivery system that could effectively transport riluzole to brain cells by reducing efflux pumps with a P-gp inhibitor, verapamil. Riluzole and verapamil cocktail liposomes were prepared by lipid film hydration. The average particle size of cocktail liposomes was 194.3 ± 6.0 nm **and their polydispersity index (PDI) was 0.272 ± 0.017 . The encapsulation efficiencies of verapamil and riluzole in the cocktail liposomes were $86.0 \pm 1.4\%$ and $85.6 \pm 1.1\%$, respectively. The drug release from cocktail liposomes after 8 hours in PBS at 37°C was $78.4 \pm 6.2\%$ of riluzole and $76.7 \pm 3.8\%$ of verapamil.** The average particle size of liposomes did not show significant changes at 4°C after three months. Verapamil cocktail liposomes inhibited P-gp levels measured by western blotting in dose and time-dependent manners in brain endothelial bEND.3 cells. Increased drug efflux transporters were detected in bEND.3 and astrocytes C8D1A cells, promoted by tumor necrosis factor (TNF- α) or hydrogen peroxide (H_2O_2). Restored accumulations of riluzole and fluorescent dye rhodamine 123 were observed in bEND.3 cells after treatments with cocktail liposomes. It indicated that inhibitory potential of co-delivery liposome system towards P-gp could mediate the transport of both P-gp substrates. Verapamil and riluzole co-loaded liposomes may be used to overcome pharmacoresistance of riluzole for improving ALS therapy.

Keywords: drug resistance, amyotrophic lateral sclerosis, verapamil, riluzole, P-gp inhibition, liposome

1. Introduction

One of the important mechanisms contributing to the clinical difficulty for the treatment of brain disorders is the obstacle from the blood-brain barrier (BBB) (Milane *et al.*, 2007; Milane *et al.*, 2009). Physiological efflux transporters, especially P-glycoprotein (P-gp), are ATP-driven efflux pumps with remarkably broad substrates. They are responsible for the inability of many xenobiotics to enter the brain (Mahringer *et al.*, 2011). They pump drugs from the brain endothelial membrane and cytosol compartment back into the blood for subsequent elimination and untargeted distribution. As a result, insufficient drug deposition in the brain leads to the failure of treatment (Mahringer *et al.*, 2011; Neuwelt *et al.*, 2011). Moreover, because the BBB is a complex and dynamic interface spontaneously responding to physiological changes, promotions of efflux transporters occur in several neurological diseases, including epilepsy, brain cancer, spinal cord injury, Alzheimer's disease, and Parkinson's disease (Mahar Doan *et al.*, 2002; Mahringer *et al.*, 2011). The overexpression of efflux transporters, constituting the major mechanism of cell adaptation to disease and environmental stress, produces more drug export (Mahringer *et al.*, 2011). Therefore, efflux transporters at the BBB not only lead to the majority of drug failures to reach clinical approval due to low uptake of potential therapeutics into the brain but also induce pharmacoresistance of approved drugs in the later stage of diseases.

Amyotrophic lateral sclerosis (ALS) is a progressive motor neuron disease. The life expectancy of an ALS patient averages 2 to 5 years from the time of diagnosis (de Carvalho *et al.*, 2005; Chio *et al.*, 2009; Mitchell *et al.*, 2010). While the Food and Drug Administration (FDA) recently approved Mitsubishi Tanabe Pharma Corp's orphan drug edaravone as the second medication in May 2017, riluzole has been the only FDA approved the medication for the treatment of ALS for more than two decades. Riluzole appears to slow the disease's progression by reducing levels of glutamate, which often presents in higher levels in ALS patients. However, riluzole is moderately effective for ALS

patients and prolongs survival by only three months (Bryson *et al.*, 1996; Bellingham, 2011). According to previous studies, increased P-gp transporter activity and expression are induced by ALS (Chan *et al.*, 2017). As riluzole is a substrate of P-gp, the inductions potentially limit the brain distribution of riluzole and further promote drug resistance in the later stage of ALS disease.

Due to the novel structure, liposomes offer an alternative delivery system for drugs to potentially enhance their *in vitro* and *in vivo* drug stability, control their release rate, and improve their delivery to the brain. Studies on liposomal antiarrhythmic verapamil have shown a noted reduction of P-gp and improved the treatment of epilepsy and cancers *in vitro* and *in vivo* (Binkhathlan & Lavasanifar, 2013). In order to address the limitations of ALS therapy, we first propose to develop a liposome that could effectively co-deliver P-gp inhibitor and riluzole to overcome pharmacoresistance and improve the distribution of riluzole in the brain. In this study, we investigated if verapamil, a traditional inhibitor of P-gp, could lead to the improved delivery of riluzole in an *in vitro* mouse brain endothelial bEND.3 and astrocyte C8D1A cells. P-gp significantly overexpressed in cells under inflammation and oxidation stimulated ALS-mimic conditions. Induced P-gp was inhibited after the treatment of optimized liposome formulations. Following the silencing of P-gp in cells, increased intracellular accumulation of P-gp substrates, rhodamine 123 and riluzole, was observed. Our results indicated that it is possible that a new strategy using a liposome-based co-delivery system can overcome the pharmacoresistance of riluzole mediated by the P-gp expression at the BBB, a particular interest in the enhancement of brain uptake of riluzole for the treatment of ALS.

2. Materials and methods

2.1 Materials

Brain endothelial bEND.3 cell, astrocyte C8D1A, Dulbecco's Modified Eagle's medium (DMEM), fetal bovine serum (FBS), penicillin plus streptomycin solution, and trypsin-EDTA were obtained from American Tissue Culture Collection (Rockville, MD, USA). Rhodamine 123, verapamil, riluzole, tumor necrosis factor alpha (TNF- α), 3% hydrogen peroxide (H₂O₂) were purchased from VWR (Radnor, PA, USA). Egg distearoylphosphatidylcholine (DSPC), cholesterol, and 1, 2-distearoyl-sn-glycero-3-phosphoethanol amine-N-[methoxy(poly ethylene glycol)-2000] (DSPE-PEG2000) were from Avanti Polar Lipids Inc. (Alabaster, AL, USA). P-gp antibody was obtained from Enzo Life Science Inc. (Farmingdale, NY, USA). Western Lightening Chemiluminescence reagents were purchased from Amersham Biosciences, Inc. (Piscataway, NJ, USA). Cell lysis buffer was purchased from Cell Signaling Technology Inc. (Boston, MA, USA). Other chemicals and reagents were purchased from VWR (Radnor, PA, USA).

2.2 Preparation of riluzole and verapamil cocktail liposomes

Liposomes of riluzole and verapamil composed of distearoylphosphatidylcholine (DSPC), cholesterol, and 1,2-distearoyl-sn-glycero-3-phosphoethanolamine-N-[methoxy(poly ethylene glycol)-2000] (DSPE-PEG2000) (molar ratio of PC: cholesterol: DSPE-PEG 2000 = 6:3:0.6; the total amount of lipid was 12.7 mg), were prepared by using a hydration method described previously (Yang *et al.*, 2014). Briefly, lipid mixtures with no drugs, 0.1 ml (20 mg/ml) riluzole alone, or 0.1 ml (20 mg/ml) verapamil and 0.1 ml (20 mg/ml) riluzole were dissolved in an organic solvent and a dried thin lipid film was prepared in a round bottom flask using a Buchi R-114 Rotavapor (Buchi Laboratories AG, Flawil, Switzerland). Subsequently, the flask was kept for 2 hours under vacuum to ensure the complete removal of residual solvent. The dry lipid film was hydrated with 2 ml of phosphate buffer solution (PBS) at a temperature of 50 \pm 2 °C. The suspension thus obtained was vortexed and dispersed in an ultrasound water bath for 5 minutes, respectively. The final formulation

was extruded through 0.4, 0.2 and 0.1 μm polycarbonate membrane filters (Coster Nucleopore, Cambridge, MA) in order. Finally, cocktail liposomes were obtained to contain 2 mg of riluzole or 2 mg of riluzole combined with 2 mg verapamil in every 2 ml of the formulation.

2.3 Particle size and size distribution determination

Particle size and size distribution measurements were performed using a Delsa™ Nano C nanosizing system working at scattering angles of 165° (Beckman Coulter, Brea, CA, USA) (Yang *et al.*, 2012; Yang *et al.*, 2014). The particle size and **polydispersity index (PDI) indicated size distribution** were analyzed by photon correlation spectroscopy, measuring the rate of fluctuations of the laser light intensity scattered by particles as they diffused through the fluid. Liposomal samples (200 μl) were dispensed into a microliter cuvette with a 100 pinhole set to 20 μm , and a refractive index of 1.3328 for 70 continuous sample accumulation times. Each analysis was repeated three times to give an average particle size of normalized intensity. The particle size was re-measured after 3 months at 4 $^\circ\text{C}$. The stability of prepared liposome formulations was evaluated by comparing the changes of average particle size (Bai *et al.*, 2007).

2.4. Drug encapsulation efficiency and release

The encapsulation efficiency of drugs in liposomes was indirectly determined from the amount of free drugs after an ultracentrifugation technique according to previous reports (Laouini *et al.*, 2011; Wang *et al.*, 2017). Briefly, riluzole or riluzole/verapamil loaded liposomes were precipitated using an XL-70 Ultracentrifuge (Beckman Coulter, Brea, CA, USA) with a 70.1 Ti rotor at 50,000 rpm for 1 hour at 4 $^\circ\text{C}$. The free drug in the supernatant was determined by a high-performance liquid chromatography (HPLC) method. The percentage of drug encapsulation efficacy was calculated from the different amount between total drug

and free drug in supernatant divided by the total amount of drug (Laouini *et al.*, 2011; Wang *et al.*, 2017).

Drug release in the liposomes was evaluated using a dialysis technique (Laouini *et al.*, 2011). A 3 ml aliquot of liposomal suspension was placed in the dialysis Cellu-Sep[®] Regenerated Cellulose Tubular Membranes with a molecular weight cut off of 20 kDa (Membrane Filtration Products Inc., Seguin, TX, USA). The dialysis bag was hermetically tied and dropped into 30 ml of PBS. The entire system was kept at 37 ± 2 °C under continuous sharking at 40 OPM in a reciprocal shaking water bath (Precision Model 50, Thermo Fisher Scientific LLC, Asheville, NC, USA). Samples (1 ml) of the dialysate were taken at various time intervals and assayed. The same volume of warmed PBS was replaced and the volume of the receptor compartment remained constant during the experiment.

Concentrations of riluzole and verapamil in supernatants were determined by a HPLC method according to a previously published and validated method (He & Wang, 2003; Saleh *et al.*, 2014). Briefly, Agilent 1220 DAD gradient HPLC system with auto-sampler and column oven was used (Agilent 1220 DAD; Santa Clara, CA, USA). Separation and quantitation were performed by using a ZORBAX C8 Column (5 μ m, 4.6 mm X 250 mm) at 40°C. The mobile phase, consisting of 0.05% formic acid in water and methanol (pH = 3.1, 70:30, v/v), was run at a constant flow rate of 1.0 ml/min. The sample injection volume was 10 μ l and **the detection wavelengths of riluzole and verapamil were set at 264 nm and 278 nm, respectively**. The method produced a linear relationship over the concentration ranging from 1 to 20 μ g/ml of riluzole and **8 to 128 μ g/ml of verapamil** ($r > 0.95$).

2.5 Cell culture and western blot analysis

Mouse brain endothelial bEND.3 and astrocyte C8D1A cells were grown in recommended Dulbecco's Modified Eagle's medium (DMEM) supplemented with 10% FBS, 2 mM L-

glutamine, 100 µg/ml penicillin plus 100 µg/ml streptomycin, in a humidified 37°C incubator with 5% CO₂ according to ATCC protocols. Proteins were isolated from the confluent bEND.3 or C8D1A cells using a cell lysis buffer. Total protein concentrations were measured with a Pierce BCA assay kit. P-gp levels in cells were analyzed by a western blotting method according to previously published procedures (Bai *et al.*, 2008). 50 µg of proteins were electrophoresed and transferred to a polyvinylidene difluoride membrane. The membranes were treated with a primary P-gp antibody and then a secondary antibody. Signals for proteins were detected by Western Lightening Chemiluminescence reagents. The P-gp protein level was quantified from the densitometric intensity of each band using a UVP ChemiDoc-It® Imager (Upland, CA, USA).

2.6 P-gp silence in brain endothelial cells

Efficacy of liposome on the inhibition of P-gp expression was tested by determining P-gp levels in P-gp highly expressed brain endothelial bEND.3 cells. Cells were seeded on a 100 mm x 15 mm Petri dishes at a density of 2x10⁶ cells/ml counted by a Cellometer® Auto T4 Cell Counter (Nexcelom Bioscience LLC, Lawrence, MA, USA). After 24 hours of cell growth in the Petri dishes, buffer solution or verapamil and riluzole liposomes was added with a series of concentrations and incubated for different times, respectively. After treatments, P-gp levels in cells were analyzed by the western blotting method as described in section 2.5. Results were normalized to total protein loading confirmed by BCA protein assay and expressed as a percentage of the band volume (the product of western band intensity and band area) of treatment compared to that derived from the buffer control (Yang *et al.*, 2014; Chan *et al.*, 2017; Yang *et al.*, 2017).

2.7 P-gp inhibition in stimulated brain cells

Increased level and activity of P-gp at the BBB are associated with the inflammatory process in brain disorders (Yin *et al.*, 2010; Erickson *et al.*, 2012). The level of P-gp expression is elevated when cells are subjected to oxidative stress induced by hydrogen

peroxide (H_2O_2) and inflammatory mediator tumor necrosis factor-alpha (TNF- α) (Lee *et al.*, 2012; Qosa *et al.*, 2016). In the study, bEND.3 and C8D1A cells were seeded on 100 mm x 15 mm Petri dishes at a density of 1×10^6 cells/ml, respectively. After 24 hours of growth, cells were treated hydrogen peroxide and TNF- α with a series of concentrations for 48 hours at 37°C and 5% CO_2 . The cells were then treated with optimized verapamil and riluzole liposome for 0 to 24 hours at 37°C and 5% CO_2 . After both sets of treatments, P-gp expression was evaluated using the Western blot method as described in section 2.5.

2.8 Rhodamine 123 uptake in brain endothelial cells

Brain endothelial bEND.3 cells were seeded on a 6-well plate with 2 ml of cell media at a density of 2×10^5 cells/ml. After 24 hours of incubation at 37°C and 5% CO_2 , two groups of cells were treated with or without 40 ng/ml TNF- α for 48 hours. And then optimized formulations including 0.2 mg/ml rhodamine 123 alone or with the optimized riluzole and verapamil cocktail liposomes (30 $\mu\text{g}/\text{ml}$) were added to the media. After 18 hours of incubation at 37°C, the media with treatment solution were removed and the cells were washed with 1 \times PBS three times. Cells were fixed in paraformaldehyde solution and permeabilized in Triton X-100. The final cell samples were imaged using an EVOS® FL cell imaging system (Life Technologies, Waltham, MA) (Yang *et al.*, 2015; Yang *et al.*, 2017).

2.9 Riluzole uptake in brain endothelial cells

Brain endothelial bEND.3 cells were seeded on a 100 mm petri dish at a density of 2×10^5 cells/ml. After 24 hours of incubation at 37°C and 5% CO_2 , two groups of cells were treated with or without 40 ng/ml TNF- α for 48 hours. And then formulations including 30 $\mu\text{g}/\text{ml}$ of riluzole and verapamil cocktail liposome, were added to the media. After 72 hours of incubation at 37°C and 5% CO_2 , the media with treatment solution were removed. The

cells were washed and then scraped. Riluzole and proteins were released from cells using cell lysis buffer. Total protein concentrations were measured with a Pierce BCA assay kit. Concentrations of riluzole in supernatants were determined by high-performance liquid chromatography as described in section 2.4. The final cell uptake of riluzole was expressed as quantity ratios of riluzole to total protein in the samples.

2.10 Statistical analysis

All values were expressed as the mean \pm SD. All sets of experiment were repeated at least 3 times. One-way ANOVA was used to compare the data. When the differences in the means were significant, post-hoc pair wise comparisons were conducted using Newman-Keuls multiple comparisons (GraphPad Prism, version 3.03, GraphPad Software, San Diego, CA). Differences in p -values less than 0.05 were considered statistically significant.

3. Results

3.1 Characterization of prepared liposomes

Riluzole and verapamil loaded liposomes were prepared by a thin-film hydration method with three types of lipids, including distearoylphosphatidylcholine, cholesterol, and polyethylene glycol 2000 linked 1,2-distearoyl-sn-glycero-3-phosphoethanolamine. **The first set of experiment was designed to evaluate if the inclusion of riluzole and verapamil could affect *in vitro* characterization in terms of particle size, size distribution, and drug encapsulation efficiency in the liposomal formulations. As shown in Table. 1, all liposomal formulations demonstrated a uniform size distribution ranging from 170 to 200 nm. The average particle size of blank liposomes was 171.1 ± 3.8 nm with a polydispersity Index (PDI) of 0.059 ± 0.025 . While there was a slight increase after the addition of riluzole in the liposomes with a particle size of 177.6 ± 4.8 nm ($p > 0.05$), their PDI (0.116 ± 0.008) in riluzole-loaded**

liposomes was significantly higher ($p < 0.05$). Upon the incorporation of both riluzole and verapamil into the liposome, there were significant increases in both particle size of 194.3 ± 6.0 nm and PDI of 0.272 ± 0.017 , when compared to the blank and riluzole alone liposomes ($p < 0.05$). The high encapsulation efficiency ($82.8 \pm 1.7\%$) was observed in riluzole alone liposomes. In the riluzole and verapamil cocktail liposomes, riluzole and verapamil encapsulation efficiencies were $85.6 \pm 1.1\%$ and $86.0 \pm 1.4\%$. Upon the incorporation of verapamil into the liposome, there was no significant decrease in riluzole encapsulation efficiency in liposomes in Table 1 ($p > 0.05$).

The physical stability of riluzole and verapamil cocktail liposomes in PBS during the storage at 4°C was studied in terms of the change of particle size. The temperature was selected based on the recommendation that most commercial liposomal formulations are refrigerated when being stored. The particle sizes of all three liposomes did not significantly change at 4°C ($p > 0.05$), suggesting that the vesicles were stable and not aggregating during three months of storage (Fig. 1). In the study, the releases of riluzole and verapamil from liposomes were rapid (about 40% of total encapsulated drug) during the first 0.5 hours. And then sustained releases of both riluzole and verapamil were observed as $78.4 \pm 6.2\%$ of riluzole and $76.7 \pm 3.8\%$ of verapamil were released after the next 8 hours (Fig. 2). This biphasic release result is in agreement with that reported by other groups in the liposome studies (Laouini *et al.*, 2011; Wang *et al.*, 2017).

3.2 P-gp silence by cocktail liposomes in brain endothelial cells

The expression of P-gp in brain endothelial bEND.3 and astrocyte C8D1A cells was first characterized using a western blotting method. The results were expected to be used as reference levels of P-gp for further studies. It was shown that P-gp expression in bEND.3 cells was 4 times higher than in C8D1A cells, with a mean density of western blotting band

of $411.0 \pm 1.7\%$ versus $100.0 \pm 10.0\%$ (**Fig. 3**). As significantly high P-gp expression was observed in brain endothelial bEND.3 cells, they were considered as a viable model to evaluate P-gp inhibition and further optimize riluzole and verapamil cocktail liposomes.

bEND.3 Cells were treated with riluzole and verapamil liposomes at different doses and time durations to determine the inhibitory levels of P-gp. In the buffer control treatment, the expression of P-gp was noted as a baseline level (100%). After the exposure to 5, 10, 20, 30, and 40 $\mu\text{g/ml}$ cocktail liposomes for 48 hours, bEND.3 cells resulted in a distinct decrease of P-gp expression with $93.0 \pm 5.2\%$, $85.8 \pm 4.7\%$, $50.3 \pm 5.6\%$, $26.2 \pm 5.1\%$, and $20.8 \pm 4.9\%$ of the baseline level, respectively (**Fig. 4**). The extent of the decrease was linearly dependent on the concentration of verapamil in formulations (5 to 30 $\mu\text{g/ml}$), while inhibited levels of P-gp by 30 $\mu\text{g/ml}$ and 40 $\mu\text{g/ml}$ of verapamil cocktail liposome were not significantly different ($p > 0.05$).

As shown in **Fig 5**, a rapid and transient decrease in P-gp levels was observed with the treatment of 30 $\mu\text{g/ml}$ verapamil cocktail liposome after 2, 4, 8, 16 and 24 hours. After 2 hours, P-gp levels were slightly below the base level ($98.4 \pm 9.1\%$) and then significantly declined to $87.8 \pm 1.5\%$, following by a dramatic decrease from 8 to 16 hours ($75.3 \pm 3.0\%$ to $43.1 \pm 2.4\%$). The liposomes resulted in the lowest suppressed levels in P-gp ($15.7 \pm 0.6\%$) at 24 hours, which was the longest time point in the study. Thus, the brain endothelial cell could rapidly respond to the P-gp inhibitor verapamil due to the application of cocktail liposomes. All the results indicated riluzole and verapamil liposomes significantly silenced P-gp in a dose and time-dependent manners.

3.3 P-gp inhibition in stimulated brain cells

After observing riluzole and verapamil cocktail liposomes could inhibit P-gp in the normal bEND.3 cells, we further investigated their effect on P-gp expression in inflammatory and oxidative stress models in both bEND.3 and C8D1A cells by western blot analysis. As shown in **Fig. 6A**, the expression of P-gp was increased in a dose-dependent manner with

the treatment of TNF- α . The highest expression of P-gp was $294.1 \pm 6.2\%$ of baseline level from the buffer control after cells were stimulated by 40 ng/ml of TNF- α . The results indicated that 30 μ g/ml verapamil cocktail liposomes could significantly reverse the increase in P-gp ($p < 0.05$). The verapamil cocktail liposomes showed stronger inhibition compared verapamil/riluzole solution with the P-gp level of $58.8 \pm 4.2\%$ versus $80.6 \pm 7.4\%$ ($p < 0.05$). The similar results were also observed in C8D1A cells, although the total expression of P-gp was much lower in the astrocyte cells (**Fig. 6B**).

The inhibitory efficacy of riluzole and verapamil cocktail liposomes on levels of P-gp was also explored in hydrogen peroxide (H_2O_2) stimulated cells. Concentration-dependent induction of P-gp protein in bEND.3 cells was clearly shown in **Fig. 7A**. The increase ($124.2 \pm 10.6\%$) of P-gp was observed at 10 μ M of H_2O_2 and continued to increase at 50 μ M ($207.7 \pm 7.9\%$). Similarly, the induction of P-gp in C8D1A cells by H_2O_2 was also detected in a dose-dependent manner. Following 48 hours of H_2O_2 (50 μ M) exposure, the expression of P-gp protein increased to $226.1 \pm 12.0\%$ (**Fig. 7B**). Consistent with the results from TNF- α stimulation study, 30 μ g/ml verapamil cocktail liposomes resulted in a significantly decreased P-gp level of $73.9 \pm 6.0\%$ ($p < 0.05$). All the results from both inflammation and oxidation stimulations indicated cocktail liposomes inhibited the overexpressed P-gp in inflammation and oxidation stimulated cells. Moreover, the cocktail liposome formulation produced better inhibition of P-gp compared to verapamil and riluzole solution.

3.4 Rhodamine 123 uptake in brain endothelial cells

In order to determine whether P-gp mediates the function of efflux and results in drug resistance, cell uptake of rhodamine 123, a P-gp substrate, was studied under both normal and TNF- α stimulated bEND.3 cells. Based on our previous studies, the optimized concentration of rhodamine 123 produced an observable intensity of fluorescence in bEND.3 cells (**Fig. 8A**). As shown in **Fig. 8B**, a significant decrease in uptake in rhodamine

123 was observed in bEND.3 cells stimulated with 40 ng/ml of TNF- α after 48 hours of exposure, when compared to normal cells. As TNF- α stimulation increased P-gp expression (**Fig. 6**), it is thus reflecting TNF- α stimulation could increase P-gp efflux function towards the fluorescent rhodamine 123 from the cells. In the presence of the reference P-gp inhibitor verapamil at a concentration of 30 μ g/ml, rhodamine 123 accumulation in stimulated cells was restored and even increased to the level found in both normal and stimulated cells (**Figs. 8C and 8D**). The data indicated that cocktail liposomes could inhibit the efflux function of overexpressed P-gp in stimulated cells.

3.5 Riluzole uptake in brain endothelial cells

As shown in **Fig. 9**, a significant decrease in riluzole accumulation was observed in TNF- α stimulated cells. In the stimulated cells, riluzole uptake to total protein was decreased (2.3 ± 0.2 μ g/mg riluzole/total protein) compared to that in the normal cells (3.0 ± 0.3 μ g/mg) ($p > 0.05$). The riluzole uptake significantly restored (4.6 ± 0.4 μ g/mg) by cocktail liposomes at concentrations of 30 μ g/ml in TNF- α stimulated bEND.3 cells. The maximum uptake of riluzole in bEND.3 cells (6.3 ± 0.5 μ g/mg) was found in the normal cells treated with 30 μ g/ml of verapamil cocktail liposomes. Overall, both normal and stimulated bEND.3 cells seemed to be sensitive to verapamil treatments. When the uptake study with 30 μ g/ml of verapamil cocktail liposomes was repeated in stimulated cells, the riluzole uptake was significantly increased, even higher than that in normal cells without stimulation ($p < 0.05$). These data together with the results of inhibition of P-gp (**Figs. 4-7**) and cell uptake of rhodamine 123 (**Fig. 8**) suggest that the inhibition of verapamil in cocktail liposome promoted the cell uptake of P-gp substrates, rhodamine 123 and riluzole.

4. Discussion

Currently, the number of people affected by brain diseases and disorders is growing at a rapid rate. Neurodegenerative disorders such as ALS, Alzheimer's disease, Huntington's

disease, and Parkinson's disease, affect more than 45 million people worldwide (Wong *et al.*, 2014). Treatment of brain diseases remains one of the biggest clinical challenges because of the difficulty of adequate delivery of therapeutic agents into the brain (Chen & Liu, 2012; Geldenhuys *et al.*, 2012; Krol, 2012). Formed by a continuous monolayer of cerebrovascular endothelial cells joined together by tight junctions, the BBB restricts the penetration into the brain not only of large molecule drugs but also more than 98% of small molecule drugs (Pardridge, 2005; Muldoon *et al.*, 2007; Tucker, 2011). In addition, the BBB expresses high levels of P-gp. Although the drugs have deposited in the brain, P-gp can pump out the drugs and cause the loss of therapeutic efficacy due to the resulted low drug amount. Moreover, the P-gp at the BBB is also responsible for the acquired drug resistance (Mahringer *et al.*, 2011). As a dynamic interface, P-gp transporters voluntarily respond to physiological changes and can even be promoted by brain diseases (Mahar Doan *et al.*, 2002; Mahringer *et al.*, 2011).

ALS is a slowly progressing neurodegenerative disease affecting motor neurons in the nervous system. Although many potential therapeutics targeting disease mechanisms are identified *in vitro*, there has been limited progress in translating them into successful therapeutic agents in the treatment of ALS in the clinic. This obstacle is primarily due to the difficulty to deliver the therapeutic agents into the brain. Before the Food and Drug Administration (FDA) recently approved orphan drug edaravone as the second medication in May 2017, riluzole is the only FDA approved the medication for the treatment of ALS, which modestly extends survival both in the animal model and in patients. However, studies in patients demonstrated that riluzole is particularly effective in the first 12 months of treatment, reducing mortality by 38%. This initial efficacy is reduced to 19.4% at 21 months of treatment because of ALS disease-driven pharmacoresistance mediated by P-gp efflux transporters (Daood *et al.*, 2008; Wang *et al.*, 2014; Chan *et al.*, 2017). Issues involved in effective riluzole treatment result from an underestimated drug bioavailability

and disease-driven pharmacoresistance, mediated by P-gp drug efflux transporters. Multiple reports have identified an increase in P-gp expression in ALS mutant mice (Milane *et al.*, 2009). An overexpression of P-gp (1.5-fold) was observed in presymptomatic mSOD1 mice compared to normal controls. Consistently, the P-gp function was also increased by 1.5-fold and riluzole brain disposition was decreased by 1.7-fold in mSOD1 mice (Chan *et al.*, 2017). These results demonstrate that BBB transport proteins are overexpressed in the ALS disease state. Thus, it is essential to reconsider the strategies for the treatment of ALS by overcoming pharmacoresistance of riluzole.

As P-gp transports drugs out of the brain and back into the blood, drug uptake in the brain can be improved by inhibiting drug efflux at the BBB (Breedveld *et al.*, 2006; Binkhathlan & Lavasanifar, 2013). Previous work to inhibit P-gp mediated drug efflux at the BBB included the use of specific inhibitors and gene knockdown (Constantinides & Wasan, 2007; Akhtar *et al.*, 2011). While the use of small interfering RNA (siRNA) to downregulate the expression of P-gp is promising, the delivery of siRNAs faces tremendous barriers before entering in the targeted cell cytoplasm. This is because negative phosphate charges and large molecular weight make siRNAs difficultly cross cellular membranes. In addition, the fragile molecular nature of siRNAs render them to rapid degradation by nucleases and result in a short circulating half-life *in vivo* (Tokatlian & Segura, 2010). P-gp modulators, including clinically used antiarrhythmic verapamil and nifedipine, have shown a noted reduction in P-gp function, although they may result in unwanted pharmacological effects (Binkhathlan & Lavasanifar, 2013). More importantly, numerous research groups have encapsulated verapamil in liposomes and reported effects on P-gp-mediated transport of co-encapsulated substrate drugs such as doxorubicin (Krishna & Mayer, 2000; McCarthy *et al.*, 2014). In order to address the limitations of ALS therapy, we first propose to develop liposome nanocarriers that could effectively co-deliver a

traditional P-gp inhibitor, verapamil, and riluzole, therefore overcoming the P-gp resistance and improving ALS therapy.

Liposomes, also called liposomal nanoparticles, are nanosized vesicles composed of a concentric lipid bilayer with an aqueous compartment as the core. The solubility of both hydrophilic and lipophilic drugs can be increased after being encapsulated in two compartments, respectively. Due to their novel structure, liposomes offer an alternative delivery system for drug delivery to improve the drug solubility, sustain the release rate of the drug, and improve the drug pharmacokinetic profiles. For example, doxorubicin given in liposomes has a half-life of 55 hours, five times longer compared to its traditional IV formulation. Although miscellaneous factors may affect the properties of liposomes, our first aim of the study was to test the difference between blank and drug-loaded liposomes. Meanwhile, two main factors, lipid amounts and particle size of liposomes, which affect the blood circulation time of loading drug, were also considered. First, the loading ratio of riluzole and verapamil was selected as 1:1 (w/w). Based on the ratio, the dose of riluzole would work in the treatment of ALS, but verapamil should not have pharmacological activity. In another regard, lipid amount and ratio were chosen according to our previous studies (Bai & Ahsan, 2010). In the study, three kinds of commonly used lipids (phosphatidylcholine, cholesterol, and PEGylated DSPE) were used to prepare long-circulation liposomes based on our experience and literature reported (Carrion *et al.*, 2001; Kim *et al.*, 2003; Bai & Ahsan, 2010). Since novel synthetic lipid derivatives of polyethylene glycol (PEG) have been reported to decrease the uptake of liposomes by the reticuloendothelial system and to prolong circulation half-lives of liposomes, we alternated DSPE to PEGylated DSPE to prepare long-circulating liposomes. **In our study, the particle size pattern was influenced by the inclusion of drugs. In the presence of verapamil, the average size and size distribution measured by PDI of PEGylated liposomes tended to be bigger (Table. 1). Generally, initially prepared liposome**

preparations are a mixture of encapsulated and free drug fractions. The feasible encapsulation efficiencies of riluzole and verapamil were believed to be due to the high lipophilicity of both drugs and therefore their good solubility in phospholipids.

Since aggregation is a physical stability indicator of liposomes, we checked if the particle size of prepared riluzole and verapamil cocktail liposome could increase at 4 °C for 3 months. PEGylated liposome with a sufficiently high surface hydrophilic groups could form steric repulsion, so the liposomes prepared in the study were stable without aggregation, which was consistent with previous studies (Hong *et al.*, 2001). Taken together, PEGylated liposomes with the inclusion of both riluzole and verapamil possessed certain stability for further studies.

At the BBB, brain endothelial cells are major components containing a monolayer with high transendothelial electrical resistance. Astrocytes extend foot-like projections to ensheath cerebral vessel. As a result, astrocytes induce the expression of the majority of barrier-specific properties in endothelial cells. They are the chief cell type responsible for BBB induction and/or maintenance (Pardridge, 2005; Muldoon *et al.*, 2007; Tucker, 2011). We first evaluated the basal levels of P-gp in mouse brain endothelial bEND.3 and astrocyte C8D1A cells using the western blotting method. As brain endothelial cells derived from the BBB tissue, bEND.3 cells have been commonly used as an *in vitro* BBB model (Wan *et al.*, 2014; Yang *et al.*, 2017). A high expression of P-gp was observed in bEND.3 cells (**Fig. 3**). This supports that the cells can be used as an *in vitro* BBB model and they are viable to evaluate the inhibition of P-gp. On the other hand, the P-gp expression was relatively weak in astrocyte C8D1A cells. In this study, we investigated whether cocktail liposomes of riluzole and verapamil could silence P-gp in dose and time-dependent manners in P-gp highly expressed bEND.3 cells. The results in **Figs. 4 and 5**, showed the treatments with increased doses and time durations of verapamil cocktail liposomes could proportionally inhibit P-gp.

Several major mechanisms of neurodegeneration in ALS, including oxidative stress, excitotoxicity, mitochondrial dysfunction, disruption of the neurofilament network, inflammation, and aggregation of proteins have been highlighted (Chio *et al.*, 2009). In this study, we developed ALS-like conditions in the brain endothelial and astrocyte cells stimulated by tumor necrosis factor (TNF)- α and hydrogen peroxide (H₂O₂), respectively. TNF- α is a proinflammatory cytokine and modulates the functions of the constituent endothelial cells. P-gp levels at the BBB are subject to regulation by TNF- α stimulated inflammation (Yu *et al.*, 2007). Oxidation causes biological changes in cells and makes the cells vulnerable to reactive oxygen species. After exposure to H₂O₂, cells highly correlate with the down-regulated expression of antioxidant genes (Yue *et al.*, 2008). The brain endothelial bEND.3 cells used in the study have been shown to highly express P-gp. The relatively high expression and up-regulation of P-gp at the BBB could provide more selectivity for evaluating the improved delivery of riluzole into the brain under ALS-mimic conditions. Because oxidative modification of P-gp significantly increases in ALS patients and inflammation is associated with oxidative stress in the brain, we determined whether similar patterns in the inflammation and oxidative modifications were present in our bEND.3 and C8D1A cells. The concentration-response curve illustrated in **Figs. 6A and 7A** showed a considerable overexpression of P-gp in both cells as the concentrations of TNF- α were increased from 10 to 40 ng/ml. Furthermore, P-gp expressions in both cells were also up-regulated with the stimulation of H₂O₂ from 10 to 50 μ M (**Figs. 6B and 7B**), which agrees with the previous report showing overexpression of P-gp in astrocytes in some brain diseases (Qosa *et al.*, 2016). Under the ALS-mimic conditions in both brain endothelial and astrocyte cells, cocktail liposome treatment significantly inhibited P-gp as shown in **Figs. 6 and 7**. More interestingly, verapamil in the cocktail liposome produced better silencing effect on P-gp compared to its solution. This agrees with previous reports that liposomes can transport encapsulated drug *via* endocytosis across the lipid cell

membrane and avoid the passive diffusion or receptor-mediated transport (Torchilin, 2005). As a result, verapamil encapsulated in the liposomes is not be pumped directly out of the cells by the P-gp, meanwhile, more drugs stay in the cells and decrease the resistance in the P-gp expressing cells (Wang *et al.*, 2011).

The cell uptake of rhodamine 123, a fluorescent P-gp substrate, was evaluated by fluorescent microscopy in bEND.3 cells. When brain endothelial cells were incubated with the co-delivery of rhodamine 123 and verapamil cocktail liposome, there was a significantly higher uptake of fluorescence, compared to the control groups (**Figs. 8**). Furthermore, the cocktail liposomes restored the uptake of rhodamine 123 in the cells, while cellular uptake was significantly decreased when the cells were stimulated by TNF- α with an overexpression of P-gp. Finally, we evaluated if cocktail liposome could increase the uptake of riluzole in brain endothelial bEND.3 cells. Following the knockdown of P-gp in the bEND.3 cells, we studied whether the silencing led to reduced efflux and increased intracellular accumulation of the P-gp substrate riluzole. It was shown that P-gp silencing by the cocktail liposome resulted in an improved delivery of riluzole, indicating that this strategy can be suitable to improve the drug delivery into the brain (**Fig. 9**).

5. Conclusion

Understanding and accounting for the contribution of efflux transporters in regards to ALS pharmacoresistance could improve the modest effects of riluzole and set forth a direction to re-evaluate previous drug disappointments in the development of therapeutics for ALS therapy. It is likely that novel drug delivery approaches can counteract the pharmacoresistance, therefore improving the therapeutic efficacy of riluzole. Results in this study first indicated that cocktail liposomes could improve the uptake of riluzole in an *in vitro* BBB cell model. Liposome characterizations included particle size stability and inhibitory effects on the expression as well as the function of P-gp. Significant increases

in the riluzole uptake have been achieved in normal and ALS-like cells. It is suggested that cocktail liposomes may be potentially developed as a delivery system for overcoming pharmacoresistance against riluzole in the treatment of ALS.

Reconsidering the treatment of ALS by inhibiting efflux transporters at the BBB is promising. However, obstacles do exist that need to be overcome to reach the maximum potential of therapeutics in the ALS treatment. Important issues that still need to be addressed include novel inhibitor screening and formulation optimization. This pilot study established *in vitro* studies on both delivery of riluzole and inhibition of P-gp using a traditional P-gp inhibitor. **Data on the further morphology, stability, pharmacokinetic properties, and safety of the formulation remain to be established. Future studies are planned to optimize new formulations using brain-targeting ligands and gene therapy tools to knockdown P-gp at the BBB.** Their long-term therapeutic efficacy will be investigated in mouse models of ALS.

References

- Akhtar, N., Ahad, A., Khar, R.K., Jaggi, M., Aqil, M., Iqbal, Z., Ahmad, F.J. & Talegaonkar, S. (2011) The emerging role of P-glycoprotein inhibitors in drug delivery: a patent review. *Expert opinion on therapeutic patents*, **21**, 561-576.
- Bai, S. & Ahsan, F. (2010) Inhalable liposomes of low molecular weight heparin for the treatment of venous thromboembolism. *Journal of pharmaceutical sciences*, **99**, 4554-4564.
- Bai, S., Thomas, C. & Ahsan, F. (2007) Dendrimers as a carrier for pulmonary delivery of enoxaparin, a low-molecular weight heparin. *Journal of pharmaceutical sciences*, **96**, 2090-2106.
- Bai, S., Yang, T., Abbruscato, T.J. & Ahsan, F. (2008) Evaluation of human nasal RPMI 2650 cells grown at an air-liquid interface as a model for nasal drug transport studies. *Journal of pharmaceutical sciences*, **97**, 1165-1178.
- Bellingham, M.C. (2011) A review of the neural mechanisms of action and clinical efficiency of riluzole in treating amyotrophic lateral sclerosis: what have we learned in the last decade? *CNS neuroscience & therapeutics*, **17**, 4-31.
- Binkhathlan, Z. & Lavasanifar, A. (2013) P-glycoprotein inhibition as a therapeutic approach for overcoming multidrug resistance in cancer: current status and future perspectives. *Current cancer drug targets*, **13**, 326-346.
- Breedveld, P., Beijnen, J.H. & Schellens, J.H. (2006) Use of P-glycoprotein and BCRP inhibitors to improve oral bioavailability and CNS penetration of anticancer drugs. *Trends in pharmacological sciences*, **27**, 17-24.
- Bryson, H.M., Fulton, B. & Benfield, P. (1996) Riluzole. A review of its pharmacodynamic and pharmacokinetic properties and therapeutic potential in amyotrophic lateral sclerosis. *Drugs*, **52**, 549-563.

- Carrion, C., Domingo, J.C. & de Madariaga, M.A. (2001) Preparation of long-circulating immunoliposomes using PEG-cholesterol conjugates: effect of the spacer arm between PEG and cholesterol on liposomal characteristics. *Chemistry and physics of lipids*, **113**, 97-110.
- Chan, G.N., Evans, R.A., Banks, D.B., Mesev, E.V., Miller, D.S. & Cannon, R.E. (2017) Selective induction of P-glycoprotein at the CNS barriers during symptomatic stage of an ALS animal model. *Neuroscience letters*, **639**, 103-113.
- Chen, Y. & Liu, L. (2012) Modern methods for delivery of drugs across the blood-brain barrier. *Advanced drug delivery reviews*, **64**, 640-665.
- Chio, A., Logroscino, G., Hardiman, O., Swingler, R., Mitchell, D., Beghi, E. & Traynor, B.G. (2009) Prognostic factors in ALS: A critical review. *Amyotrophic lateral sclerosis : official publication of the World Federation of Neurology Research Group on Motor Neuron Diseases*, **10**, 310-323.
- Constantinides, P.P. & Wasan, K.M. (2007) Lipid formulation strategies for enhancing intestinal transport and absorption of P-glycoprotein (P-gp) substrate drugs: in vitro/in vivo case studies. *Journal of pharmaceutical sciences*, **96**, 235-248.
- Daood, M., Tsai, C., Ahdab-Barmada, M. & Watchko, J.F. (2008) ABC transporter (P-gp/ABCB1, MRP1/ABCC1, BCRP/ABCG2) expression in the developing human CNS. *Neuropediatrics*, **39**, 211-218.
- de Carvalho, M., Costa, J. & Swash, M. (2005) Clinical trials in ALS: a review of the role of clinical and neurophysiological measurements. *Amyotrophic lateral sclerosis and other motor neuron disorders : official publication of the World Federation of Neurology, Research Group on Motor Neuron Diseases*, **6**, 202-212.
- Erickson, M.A., Dohi, K. & Banks, W.A. (2012) Neuroinflammation: a common pathway in CNS diseases as mediated at the blood-brain barrier. *Neuroimmunomodulation*, **19**, 121-130.

- Geldenhuys, W.J., Allen, D.D. & Bloomquist, J.R. (2012) Novel models for assessing blood-brain barrier drug permeation. *Expert opinion on drug metabolism & toxicology*, **8**, 647-653.
- He, L. & Wang, S. (2003) Pharmacokinetic behavior and tissue distribution of verapamil and its enantiomers in rats by HPLC. *Archives of pharmacal research*, **26**, 763-767.
- Hong, M.S., Lim, S.J., Lee, M.K., Kim, Y.B. & Kim, C.K. (2001) Prolonged blood circulation of methotrexate by modulation of liposomal composition. *Drug delivery*, **8**, 231-237.
- Kim, J.K., Choi, S.H., Kim, C.O., Park, J.S., Ahn, W.S. & Kim, C.K. (2003) Enhancement of polyethylene glycol (PEG)-modified cationic liposome-mediated gene deliveries: effects on serum stability and transfection efficiency. *The Journal of pharmacy and pharmacology*, **55**, 453-460.
- Krishna, R. & Mayer, L.D. (2000) Multidrug resistance (MDR) in cancer. Mechanisms, reversal using modulators of MDR and the role of MDR modulators in influencing the pharmacokinetics of anticancer drugs. *Eur J Pharm Sci*, **11**, 265-283.
- Krol, S. (2012) Challenges in drug delivery to the brain: nature is against us. *Journal of controlled release : official journal of the Controlled Release Society*, **164**, 145-155.
- Laouini, A., Jaafar-Maalej, C., Sfar, S., Charcosset, C. & Fessi, H. (2011) Liposome preparation using a hollow fiber membrane contactor--application to spironolactone encapsulation. *Int J Pharm*, **415**, 53-61.
- Lee, N.Y., Rieckmann, P. & Kang, Y.S. (2012) The Changes of P-glycoprotein Activity by Interferon-gamma and Tumor Necrosis Factor-alpha in Primary and Immortalized Human Brain Microvascular Endothelial Cells. *Biomolecules & therapeutics*, **20**, 293-298.
- Mahar Doan, K.M., Humphreys, J.E., Webster, L.O., Wring, S.A., Shampine, L.J., Serabjit-Singh, C.J., Adkison, K.K. & Polli, J.W. (2002) Passive permeability and P-

- glycoprotein-mediated efflux differentiate central nervous system (CNS) and non-CNS marketed drugs. *The Journal of pharmacology and experimental therapeutics*, **303**, 1029-1037.
- Mahringer, A., Ott, M., Reimold, I., Reichel, V. & Fricker, G. (2011) The ABC of the blood-brain barrier - regulation of drug efflux pumps. *Current pharmaceutical design*, **17**, 2762-2770.
- McCarthy, M., Auda, G., Agrawal, S., Taylor, A., Backstrom, Z., Mondal, D., Moroz, K. & Dash, S. (2014) In vivo anticancer synergy mechanism of doxorubicin and verapamil combination treatment is impaired in BALB/c mice with metastatic breast cancer. *Exp Mol Pathol*, **97**, 6-15.
- Milane, A., Fernandez, C., Vautier, S., Bensimon, G., Meininger, V. & Farinotti, R. (2007) Minocycline and riluzole brain disposition: interactions with p-glycoprotein at the blood-brain barrier. *Journal of neurochemistry*, **103**, 164-173.
- Milane, A., Vautier, S., Chacun, H., Meininger, V., Bensimon, G., Farinotti, R. & Fernandez, C. (2009) Interactions between riluzole and ABCG2/BCRP transporter. *Neuroscience letters*, **452**, 12-16.
- Mitchell, J.D., Callagher, P., Gardham, J., Mitchell, C., Dixon, M., Addison-Jones, R., Bennett, W. & O'Brien, M.R. (2010) Timelines in the diagnostic evaluation of people with suspected amyotrophic lateral sclerosis (ALS)/motor neuron disease (MND)--a 20-year review: can we do better? *Amyotrophic lateral sclerosis : official publication of the World Federation of Neurology Research Group on Motor Neuron Diseases*, **11**, 537-541.
- Muldoon, L.L., Soussain, C., Jahnke, K., Johanson, C., Siegal, T., Smith, Q.R., Hall, W.A., Hynnen, K., Senter, P.D., Peereboom, D.M. & Neuwelt, E.A. (2007) Chemotherapy delivery issues in central nervous system malignancy: a reality

- check. *Journal of clinical oncology : official journal of the American Society of Clinical Oncology*, **25**, 2295-2305.
- Neuwelt, E.A., Bauer, B., Fahlke, C., Fricker, G., Iadecola, C., Janigro, D., Leybaert, L., Molnar, Z., O'Donnell, M.E., Povlishock, J.T., Saunders, N.R., Sharp, F., Stanimirovic, D., Watts, R.J. & Drewes, L.R. (2011) Engaging neuroscience to advance translational research in brain barrier biology. *Nature reviews. Neuroscience*, **12**, 169-182.
- Pandya, R.S., Zhu, H., Li, W., Bowser, R., Friedlander, R.M. & Wang, X. (2013) Therapeutic neuroprotective agents for amyotrophic lateral sclerosis. *Cellular and molecular life sciences : CMLS*, **70**, 4729-4745.
- Pardridge, W.M. (2005) Molecular biology of the blood-brain barrier. *Molecular biotechnology*, **30**, 57-70.
- Qosa, H., Lichter, J., Sarlo, M., Markandaiah, S.S., McAvoy, K., Richard, J.P., Jablonski, M.R., Maragakis, N.J., Pasinelli, P. & Trotti, D. (2016) Astrocytes drive upregulation of the multidrug resistance transporter ABCB1 (P-Glycoprotein) in endothelial cells of the blood-brain barrier in mutant superoxide dismutase 1-linked amyotrophic lateral sclerosis. *Glia*, **64**, 1298-1313.
- Saleh, O.A., El-Azzouny, A.A., Aboul-Enein, H.Y. & Badawey, A.M. (2014) Riluzole: validation of stability-indicating HPLC, D1 and DD1 spectrophotometric assays. *J Chromatogr Sci*, **52**, 539-546.
- Tokatlian, T. & Segura, T. (2010) siRNA applications in nanomedicine. *Wiley interdisciplinary reviews. Nanomedicine and nanobiotechnology*, **2**, 305-315.
- Torchilin, V.P. (2005) Recent advances with liposomes as pharmaceutical carriers. *Nature reviews. Drug discovery*, **4**, 145-160.
- Tucker, I.G. (2011) Drug delivery to the brain via the blood-brain barrier: a review of the literature and some recent patent disclosures. *Therapeutic delivery*, **2**, 311-327.

- Wan, W.B., Cao, L., Liu, L.M., Kalionis, B., Chen, C., Tai, X.T., Li, Y.M. & Xia, S.J. (2014) EGb761 provides a protective effect against Abeta1-42 oligomer-induced cell damage and blood-brain barrier disruption in an in vitro bEnd.3 endothelial model. *PLoS One*, **9**, e113126.
- Wang, H., Zhao, Y., Wu, Y., Hu, Y.L., Nan, K., Nie, G. & Chen, H. (2011) Enhanced anti-tumor efficacy by co-delivery of doxorubicin and paclitaxel with amphiphilic methoxy PEG-PLGA copolymer nanoparticles. *Biomaterials*, **32**, 8281-8290.
- Wang, M., Lee, R.J., Bi, Y., Li, L., Yan, G., Lu, J., Meng, Q., Teng, L. & Xie, J. (2017) Transferrin-conjugated liposomes loaded with novel dihydroquinoline derivatives as potential anticancer agents. *PloS one*, **12**, e0186821.
- Wang, X., Campos, C.R., Peart, J.C., Smith, L.K., Boni, J.L., Cannon, R.E. & Miller, D.S. (2014) Nrf2 upregulates ATP binding cassette transporter expression and activity at the blood-brain and blood-spinal cord barriers. *The Journal of neuroscience : the official journal of the Society for Neuroscience*, **34**, 8585-8593.
- Wong, T.Y., Ferreira, A., Hughes, R., Carter, G. & Mitchell, P. (2014) Epidemiology and disease burden of pathologic myopia and myopic choroidal neovascularization: an evidence-based systematic review. *American journal of ophthalmology*, **157**, 9-25.
- Yang, T., Bantegui, T., Pike, K., Bloom, R., Phipps, R. & Bai, S. (2014) In vitro evaluation of optimized liposomes for delivery of small interfering RNA. *Journal of liposome research*, **24**, 270-279.
- Yang, T., Fogarty, B., LaForge, B., Aziz, S., Pham, T., Lai, L. & Bai, S. (2017) Delivery of Small Interfering RNA to Inhibit Vascular Endothelial Growth Factor in Zebrafish Using Natural Brain Endothelia Cell-Secreted Exosome Nanovesicles for the Treatment of Brain Cancer. *The AAPS journal*, **19**, 475-486.
- Yang, T., Martin, P., Fogarty, B., Brown, A., Schurman, K., Phipps, R., Yin, V.P., Lockman, P. & Bai, S. (2015) Exosome delivered anticancer drugs across the blood-brain

- barrier for brain cancer therapy in Danio rerio. *Pharmaceutical research*, **32**, 2003-2014.
- Yang, T., Nyiawung, D., Silber, A., Hao, J., Lai, L. & Bai, S. (2012) Comparative studies on chitosan and polylactic-co-glycolic acid incorporated nanoparticles of low molecular weight heparin. *AAPS PharmSciTech*, **13**, 1309-1318.
- Yin, K., Liao, D.F. & Tang, C.K. (2010) ATP-binding membrane cassette transporter A1 (ABCA1): a possible link between inflammation and reverse cholesterol transport. *Mol Med*, **16**, 438-449.
- Yu, C., Kastin, A.J., Tu, H., Waters, S. & Pan, W. (2007) TNF activates P-glycoprotein in cerebral microvascular endothelial cells. *Cell Physiol Biochem*, **20**, 853-858.
- Yue, G., Shi, G., Azaro, M.A., Yang, Q., Hu, G., Luo, M., Yin, K., Nagele, R.G., Fine, D.H., Yang, J.M. & Li, H. (2008) Lipopolysaccharide (LPS) potentiates hydrogen peroxide toxicity in T98G astrocytoma cells by suppression of anti-oxidative and growth factor gene expression. *BMC Genomics*, **9**, 608.

Table 1. Properties of prepared liposomes

Name	Particle Size	PDI	Encapsulation Efficiency
Blank liposome	171.1±3.8 nm	0.059±0.025	-----
Riluzole liposome	177.6±4.8 nm	0.116±0.008	82.8±1.7%
Riluzole and Verapamil liposome	194.3±6.0 nm*	0.272±0.017*	85.6±1.1% (Riluzole) [†] 86.0±1.4% (Verapamil)

PDI: polydispersity index; *p<0.05 compared to riluzole liposomes; [†]p>0.05 compared to riluzole liposomes

Figure legends

Figure 1. Particle stability of liposomes at 4°C by monitoring the average particle size in (I) bland liposomes, (II) riluzole liposomes, and (III) riluzole and verapamil liposomes (*indicated the significant difference among groups, $p < 0.05$).

Figure 2. Percentage of released drugs in riluzole and riluzole with verapamil cocktail liposomes.

Figure 3. Western blot results of P-gp expression (percentage compared to C8D1A) in (I) astrocyte C8D1A and (II) brain endothelial bEND.3 cells (*indicated the significant difference between groups, $p < 0.05$).

Figure 4. Dose-dependent study on the amount of P-gp expression (percentage compared to the buffer control) in bEND.3 cells after treatments of (I) buffer, (II) 5 µg/ml verapamil cocktail liposome, (III) 10 µg/ml verapamil cocktail liposome, (IV) 20 µg/ml verapamil cocktail liposome, (V) 30 µg/ml verapamil cocktail liposome, and (VI) 40 µg/ml verapamil cocktail liposome for 48 hours (*indicated the significant difference among groups, $p < 0.05$).

Figure 5. Time-dependent study on the amount of P-gp expression (percentage compared to the buffer control after 24 hours) in bEND.3 cells after treatments of 30 µg/ml verapamil cocktail liposomes at (I) 0 hour, (II) 2 hours, (III) 4 hours, (IV) 8 hours, (V) 16 hours, and (VI) 24 hours (*indicated the significant difference among groups, $p < 0.05$).

Figure 6. P-gp inhibition under TNF-α stimulation (percentage compared to the buffer control) in (A) brain endothelial bEND.3 and (B) astrocyte C8D1A treated by (I) buffer, (II)

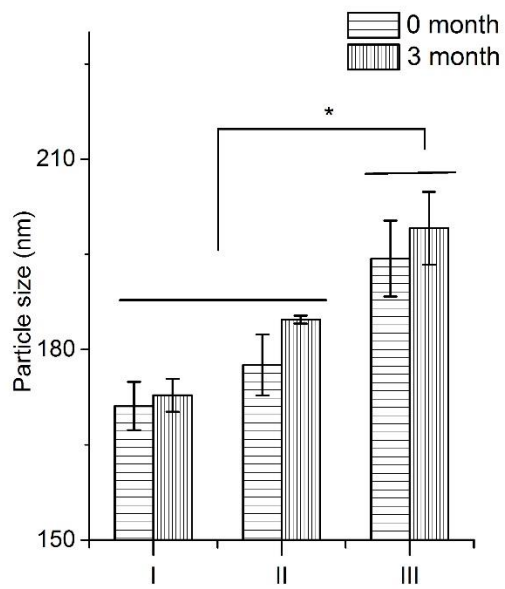
10 ng/ml TNF- α , (III) 20 ng/ml TNF- α , (IV) 30 ng/ml TNF- α , (V) 40 ng/ml TNF- α , (VI) 40 ng/ml TNF- α plus 30 μ g/ml riluzole with verapamil solution, and (VII) 40 ng/ml TNF- α plus 30 μ g/ml verapamil cocktail liposome (*indicated the significant difference among groups, $p < 0.05$).

Figure 7. P-gp inhibition under hydrogen peroxide stimulation (percentage compared to the buffer control) in (A) brain endothelial bEND.3 and (B) astrocyte C8D1A treated by (I) buffer, (II) 10 μ M H₂O₂, (III) 20 μ M H₂O₂, (IV) 30 μ M H₂O₂, (V) 40 μ M H₂O₂, (VI) 50 μ M H₂O₂, (VII) 50 μ M H₂O₂ plus 30 μ g/ml riluzole with verapamil solution, and (VIII) 50 μ M H₂O₂ plus 30 μ g/ml verapamil cocktail liposome. (*indicated the significant difference among groups, $p < 0.05$).

Figure 8. Fluorescent imaging of rhodamine 123 in (A) normal bEND.3 cells, (B) 40 ng/ml TNF- α stimulated bEND.3 cells, (C) normal bEND.3 cells treated by 30 μ g/ml verapamil cocktail liposome, and (D) 40 ng/ml TNF- α stimulated bEND.3 cells treated by 30 μ g/ml verapamil cocktail liposome.

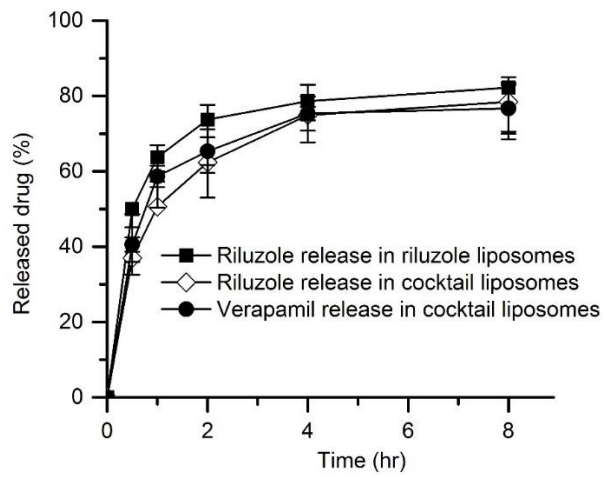
Figure 9. Riluzole uptake in (I) normal bEND.3 cells treated by 30 μ g/ml riluzole solution, (II) normal bEND.3 cells treated by 30 μ g/ml riluzole and verapamil cocktail liposome, (III) 40 ng/ml TNF- α stimulated bEND.3 cells treated by 30 μ g/ml riluzole solution, and (III) 40 ng/ml TNF- α stimulated bEND.3 cells treated by 30 μ g/ml riluzole and verapamil cocktail liposome (*indicated the significant difference among groups, $p < 0.05$).

Figure 1



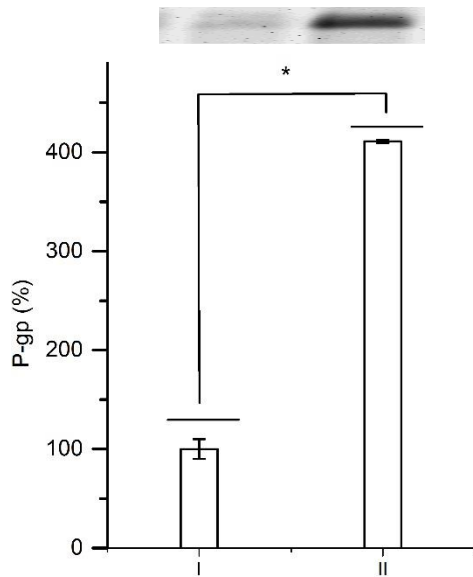
ACCEPTED MANUSCRIPT

Figure 2



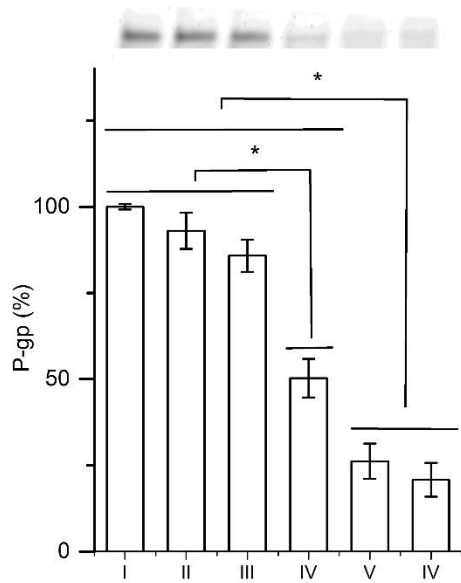
ACCEPTED MANUSCRIPT

Figure 3



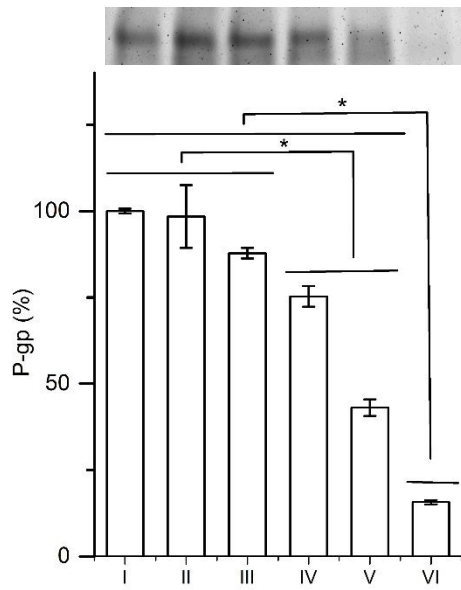
ACCEPTED MANUSCRIPT

Figure 4



ACCEPTED MANUSCRIPT

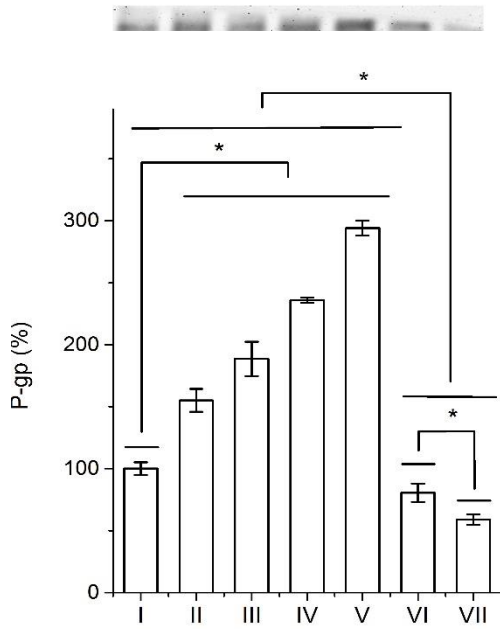
Figure 5



ACCEPTED MANUSCRIPT

Figure 6

A



B

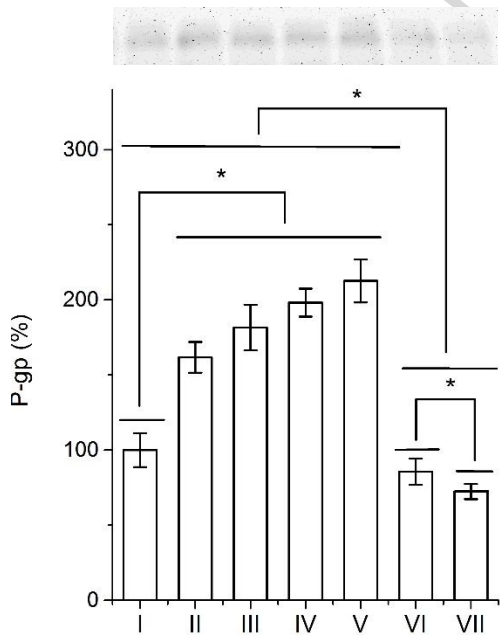


Figure 7

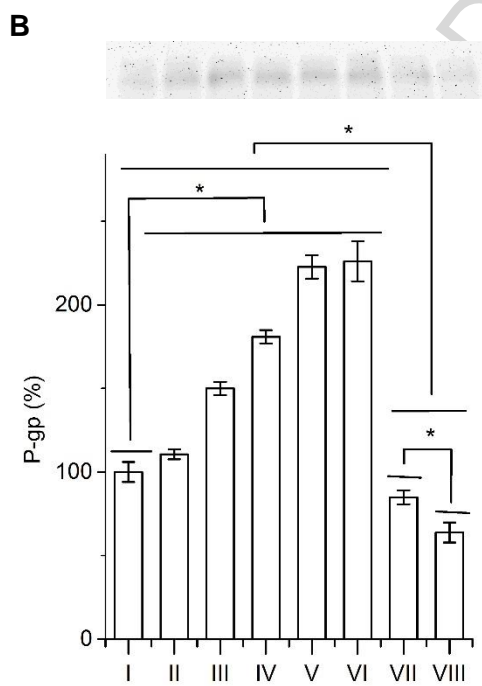
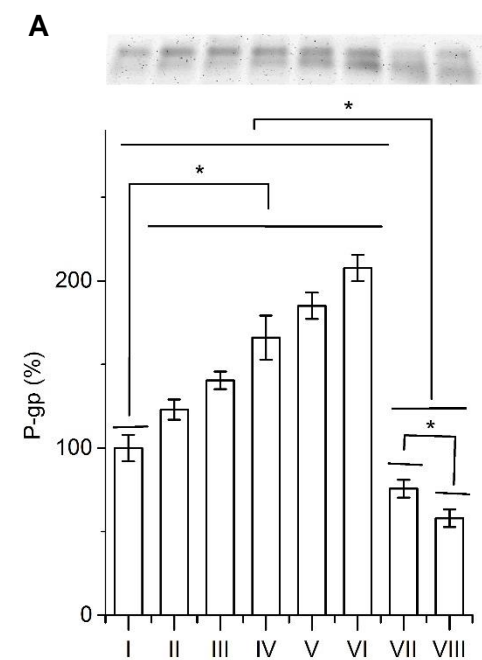
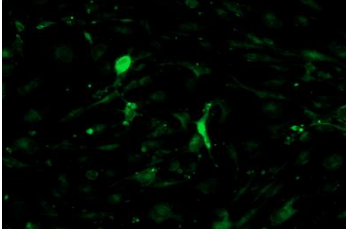
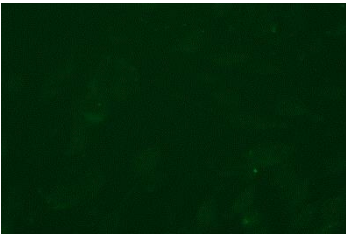


Figure 8

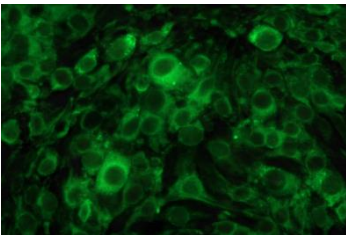
A



B



C



D

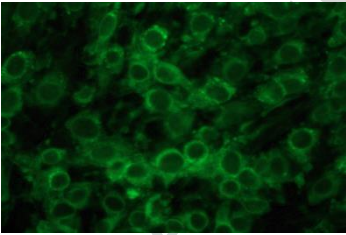
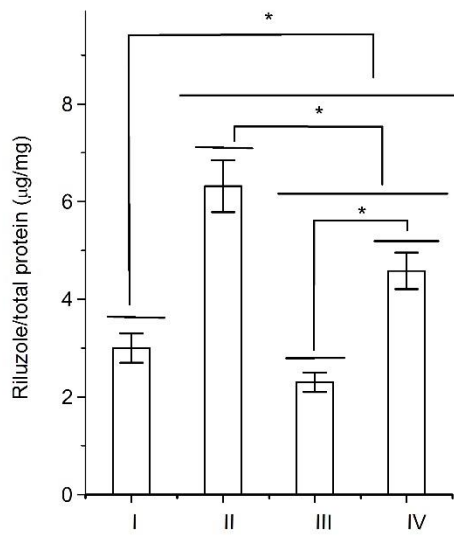
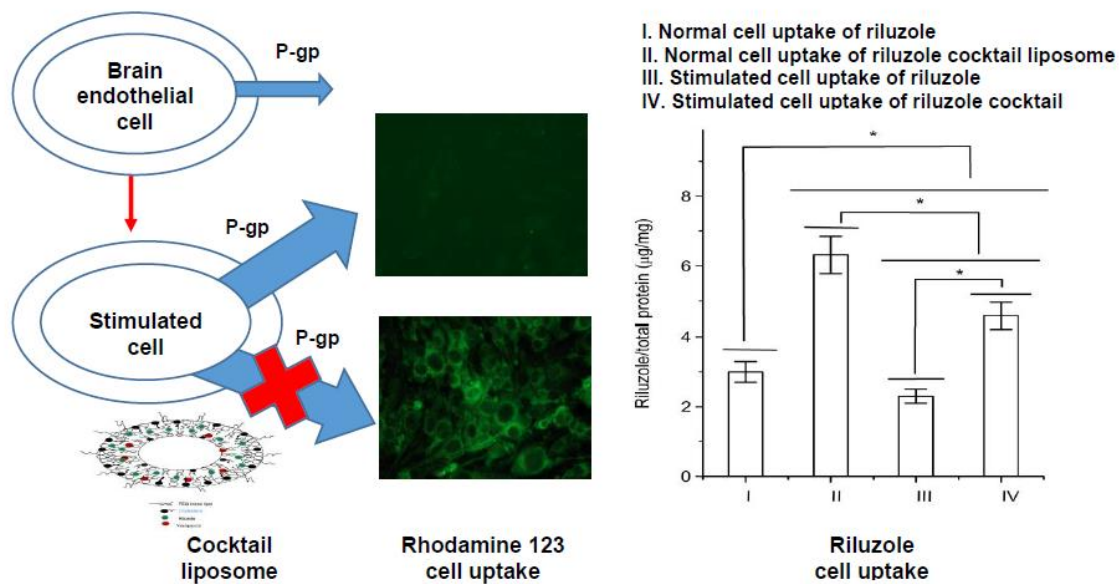


Figure 9



ACCEPTED MANUSCRIPT

Graphical abstract



ACCEPTED MANUSCRIPT